

AD-A266 407



**Evaluation of Hemoglobin-Oxygen Equilibrium Binding by Rapid-Scanning
Spectrophotometry and Singular-Value Decomposition**

DTIC
ELECTE
JUL 02 1993
S A D

Kim D. Vandegriff¹ and Richard I. Shrager²

This document has been approved
for public release and sale; its
distribution is unlimited.

93-15143



39
pgs

93 7 01 08 8

¹ Division of Blood Research, Letterman Army Institute of Research, Presidio of San Francisco, California 94129-6800

² Physical Sciences Laboratory, Division of Computer Research and Technology, Building 12A, Room 2007, National Institutes of Health, Bethesda, Maryland 20892

Detailed knowledge of the interaction between oxygen and hemoglobin is essential both for understanding oxygen transport phenomena and for testing theories of protein structure and function. The equilibrium reaction is measured routinely simply to estimate the position and shape of the oxygen binding curve from, respectively, the oxygen pressure at half-saturation (P_{50}) and the index of cooperativity (*i.e.*, the Hill number, n), but thermodynamic analysis of individual binding steps is more difficult because of inherent complexities in the reaction. For example, the linearity of optical absorption with hemoglobin fractional saturation must be assumed in the absence of analytical tools to prove it. To test this assumption and to extract more information from a single experiment, we are developing techniques using rapid-scanning spectrophotometry to measure complete spectra of hemoglobin during an oxygen binding reaction and singular-value decomposition to resolve individual components in the transition. From these analyses, models of the equilibrium reaction are being derived using laws of mass action and matrix least squares.

BACKGROUND

The reversible chemical reaction between oxygen and hemoglobin has been examined for over a century. Even though experimental methods have evolved during this time from simple gasometry to more sophisticated techniques in spectrophotometry, the reaction is still difficult to measure precisely or to interpret reliably.

The first mathematical formulation of the equilibrium was derived by Adair as a mass-action equation, with equilibrium constants describing each of the four binding steps of oxygen with the hemoglobin tetramer,¹

Availability Codes	
Dist	Avail and/or Special
A-1	

$$Y = \frac{0.25a_1x + 0.5a_2x^2 + 0.75a_3x^3 + a_4x^4}{1 + a_1x + a_2x^2 + a_3x^3 + a_4x^4} \quad (1)$$

where Y is fractional saturation, a_1 through a_4 are the overall Adair constants (*i.e.*, the product of step-wise equilibrium constants, K_1 to K_4), and x is the partial pressure of oxygen (pO_2) in solution.

The hemoglobin binding reaction was described later by allosteric theory as an equilibrium between two end-state quaternary conformations, one corresponding to the structure of deoxyhemoglobin with low oxygen affinity (*i.e.*, the T state) and the other corresponding to the structure of oxyhemoglobin with high oxygen affinity (*i.e.*, the R state).² This model has been useful particularly in the interpretation of the structural-functional mechanism of hemoglobin cooperativity,³ but it is limited in that it predicts strictly a two-state system. Recently, partially liganded species of hemoglobin have been identified with reaction energetics intermediate to the two end states but with quaternary structures still in either T or R conformation.⁴

Partially liganded intermediates are central to the mechanism of cooperative oxygen binding, but they are particularly difficult to measure because their low levels during the reaction⁵ result in a highly sigmoid binding curve. Precise measurements have been accomplished,^{6,7} but the mechanism of molecular cooperativity remains controversial. The difficulty originates from the oxygenation reaction itself, *e.g.*, the low level of partially liganded intermediates combined perhaps with differences in the reactivity of the α and β subunits^{8,9} and/or spectral changes associated with the transition between low- and high-affinity forms.¹⁰⁻¹⁵ In addition, at least two other reactions can complicate interpretation of binding data: (1) dissociation of the $\alpha_2\beta_2$ tetramer into non-cooperative $\alpha\beta$ dimers^{6,16} and (2) the redox reaction of the heme iron atoms, in which

an oxygen-binding ferrous (Fe^{2+}) heme is oxidized to a non-oxygen-binding ferric (Fe^{3+}) heme. Experimentally, these latter effects can be limited by using a hemoglobin concentration as high as possible to minimize the effects of dimers and by performing the experiment as quickly as possible or in the presence of a methemoglobin-reducing system to minimize the effects of oxidation.^{17,18}

Survey of techniques

Gasometry provides an accurate method for obtaining single points along the oxygen binding curve. This technique does not require a physical measurement of the oxyhemoglobin complex, rather, the volume of bound oxygen is measured directly. The disadvantages of using this technique are that experience and skill determine the precision of the experiment, a separate and precise measurement must be made of hemoglobin concentration, and the experiment is long and tedious. That is, the number of experimental points along a single curve depends on the number of gasometric readings that can be made on a single sample, with each reading taking ~15 minutes. Thus, for example, an experimental curve with only 10 data points takes at least 4 hours to complete: time to equilibrate 10 tonometers, each with the hemoglobin solution at a different $p\text{O}_2$, and a minimum of 150 minutes for the gasometric readings. During this interval, the hemoglobin solution will be autooxidizing, and protein degradation may occur.

Optical spectroscopy is now usually the experimental method of choice because of its speed and simplicity, and because the reaction produces a large spectral change based on hemoglobin concentration. Spectrophotometry has been combined with tonometry for expediency (*i.e.*, a hemoglobin spectrum can be recorded faster than a gasometric reading can be made).

However, like the gasometric method, time is taken for equilibration, using either separate tonometers for each data point or a single tonometer or reaction cell that is equilibrated step-wise at increasing pO_2 . In either case, the number of data points that can be measured along each curve is limited, and the experiment is still time-consuming. The primary advantage of using tonometry is that equilibrium is verified at each step (*i.e.*, at each data point) along the curve.

In contrast to tonometry, the automatic method of Imai was developed to monitor the absorbance of a hemoglobin solution as pO_2 changed continuously.^{7,19} This not only produced an equilibrium curve rapidly (*e.g.*, typically 20-60 minutes for native human hemoglobin, depending on solution conditions), thus limiting the effects of methemoglobin formation, but also provided a large number of data points along each curve. Fractional saturation of hemoglobin is calculated directly from the spectral change of the hemoglobin solution, and pO_2 is measured polarographically using an oxygen electrode mounted in the reaction chamber. However, with the continuous method, unlike tonometry, equilibrium must be assumed at each measurement point along the curve, or the reverse curve must be measured to demonstrate exact reproducibility,¹⁹ which is impossible if any oxidation has occurred. Also, because the reaction happens faster than non-rapid-scanning spectrophotometers can scan a spectral region, the transition is usually followed at a single wavelength. As with any two-state model, analysis at a single wavelength requires the further assumption that the spectral change is linearly correlated with hemoglobin fractional saturation. For the linear relation to hold, a single optical transition with a constant extinction coefficient for each binding step must take place that, in this case, would represent the transition from deoxy- to oxyhemoglobin. The actual experiment will be more complex if other reactions, such as dimer or methemoglobin formation, also occur.

There is experimental evidence both in support of and in conflict with the linear optical assumption,²⁰⁻²² with recent measurements showing that true isosbestic behavior is not maintained during the hemoglobin oxygenation reaction.^{23,24} Non-linear optical effects have been reported from both diode-array spectrophotometry, using the thin-layer tonometry method,²⁵ and a two-wavelength analysis of stopped-flow reactions by rapid mixing of oxyhemoglobin and deoxymyoglobin.²⁶

In another chapter in this volume, a technique is described that measures oxygen equilibrium binding of concentrated hemoglobin solutions non-optically, thus avoiding the issue of non-linear spectral events.²⁷ In this chapter, we describe a method based on rapid-scanning spectrophotometry to resolve directly unique optical transitions during continuous hemoglobin oxygenation. The rapid-scanning method has revealed small but significant spectral changes during oxygenation in addition to the large spectral difference from the primary transition of deoxy- to oxyhemoglobin.²⁸

The overall utility of rapid-scanning techniques will depend on two factors:

- Scanning rates must be fast enough to capture a complete spectrum of hemoglobin at a given pO_2 during the collection period. However, even at the fastest scanning rates, time elapses during the measurement, and because of this, we refer to these as "pseudoequilibrium" measurements to distinguish the possibility of kinetic events.
- The optical spectrum must have high precision to resolve small spectral changes from the large oxy-deoxyhemoglobin spectral difference.

Spectrophotometers are becoming faster, although whether they are becoming more precise is debatable. Research has pushed this technology to the limit, and new questions are demanding

the best signals that these instruments can provide. In parallel with the increasing speed of spectrophotometers, sophisticated analytical tools for data reduction are evolving, and high-speed personal computers with large memory capacities are available for the first time that can handle the huge data arrays and computational requirements of these experiments. Here we outline methods for the collection and analysis of hemoglobin spectral matrices during a "pseudoequilibrium" oxygenation reaction. Mathematical techniques for matrix multicomponent analysis and singular-value decomposition (SVD) are described, and spectral artifacts that are resolved by these sensitive techniques are discussed.

INSTRUMENTATION

We have used an LT Quantum 1200 rapid-scanning spectrophotometer (LT Industries, Inc., Rockville, MD) to obtain complete visible spectra of hemoglobin solutions during continuous oxygenation reactions. This instrument uses a tungsten-halogen light source and a rapidly oscillating grating that scans over the 400-800-nm range in 200 ms. During this 200 ms, a 70-ms dark period is allowed for instrument calibration. The light is then exposed to the monochromator for 130 ms, during which time the entire range of 400-800 nm is scanned in 80 ms. From this range, we isolate the portion of the spectrum from 480-650 nm, which is collected in ~34 ms, for data analysis. To improve the signal-to-noise ratio, at least four scans are collected per data point to produce a single, averaged spectrum with a time resolution of 800 ms. The averaged scans are collected in alternating wavelength directions, with an equal number of scans in the high-to-low (800- to 400-nm) and low-to-high (400- to 800-nm) range. The instrument is calibrated such that the scans taken in either direction are indistinguishable at

equilibrium. However, instrumental noise in both the vertical, or amplitude, spectral signal (*i.e.*, due to noise in detector gain) and in the horizontal, or wavelength, position (*i.e.*, due to slight inaccuracies in the reproducibility of wavelength position from scan to scan) produces spectral artifacts that must be accounted for in the final analysis.

A schematic diagram of the experimental apparatus is shown in Fig. 1. A temperature-controlled sample holder was designed to hold a custom-made reaction cuvette having a 1-cm light path and a fused side port for a polarographic oxygen probe (Yellow Springs Instruments, Model 5331, Yellow Springs, OH). Ultra-pure gas (*i.e.*, >99.999% purity nitrogen or oxygen in a 1:1 O₂/N₂ mixture), humidified by bubbling in water at the same temperature as that circulated around the reaction cell, is introduced into the gas space at the top of the reaction cell through a needle inserted in a gas-tight septum. Venting takes place through a second needle in the septum. The solution is mixed continuously by a small, magnetic bar spinning just beneath the tip of the oxygen probe. (Stirring provides adequate mixing but can cause mechanical stress on the protein, and evidence of protein denaturation must be monitored during the reaction.)

The photodetector signal of the light passing through the cuvette is digitized for output by a 16-bit analog-to-digital (A/D) board in a computerized data collection system. The voltage signal from the oxygen electrode is amplified (Yellow Springs Instruments, Model 5300 Biological Oxygen Monitor), filtered digitally, and relayed to a second 16-bit A/D board in a second computerized data collection system. (Alternatively, a single computer with true multi-tasking capabilities could be used to collect the two signals simultaneously.) The digital filter of the oxygen voltage signal increases the signal-to-noise ratio without changing the time constant of the oxygen probe. The time constant of the oxygen probe is calculated by collecting the

transient signal from a rapid change in solution pO_2 with and without the filter in line and fitting the relaxation to an exponential equation. For the binding experiments, the relaxation time of the electrode must be faster than the change in pO_2 of the solution so that readings will reflect the true equilibrium value of pO_2 .

Data collection is under software control. At the initiation and end of a single averaged spectral data set, transistor-transistor logic (TTL) pulses are sent from the computer controller of the spectrophotometer to the A/D board designated for oxygen voltage readings. During the time between TTL pulses, the oxygen signal is collected at a specific sampling frequency. For example, at a frequency of 120 Hz, with four spectral scans averaged at 200 ms/scan, 96 oxygen voltage readings are accumulated and averaged to give a single pO_2 reading corresponding in time to the average spectrum of hemoglobin collected over the 0.8-s period.

The voltage output from the oxygen electrode is converted to mm Hg from calibration of the output to the relative percent of oxygen in air-saturated buffer at the barometric pressure in the laboratory with a correction for the water vapor pressure at the temperature of the experiment.

METHOD OF EXPERIMENTATION

The experiment is begun by bubbling pure N_2 gas through the reaction buffer in the sample cell. Deoxygenation of the buffer is monitored by the oxygen electrode. At the same time, a concentrated solution of hemoglobin (*i.e.*, >2 mM in heme) is deoxygenated separately in a temperature-controlled, spinning tonometer under a N_2 atmosphere (Instrumentation Laboratory, Model 237, Lexington, MA). Once deoxygenation is complete, the N_2 gas flow is directed above the surface of the fluid in the reaction cell, and deoxyhemoglobin is transferred

from the tonometer to the reaction cell by a gas-tight syringe that has been flushed previously with pure N_2 gas. The hemoglobin sample is diluted in the deoxygenated buffer in the sample cell, and the oxygen voltage is monitored to assure that no oxygen was introduced during the transfer. An initial spectrum is taken to verify the concentration of deoxyhemoglobin in the reaction cell; typically, concentrations of 60-200 μM in heme are used to provide an adequate optical signal and to minimize the effect of tetramer dissociation on the measurement. Lower concentrations of hemoglobin might be used to test the consequence of tetramer dissociation on the spectral transition or to monitor the reaction in the Soret region of the spectrum. We are unable to use higher (*i.e.*, ~ 1 mM) heme concentrations because the upper limit of absorbance detection is set by the fixed path length of the reaction cell.

Oxygenation is begun by switching gas valves from N_2 to 50% O_2 . The flow rate is controlled by a gas-flow controller (Matheson, Model 4360, Newark, CA) to provide a gentle stream of humidified gas over the surface of the hemoglobin solution. (Direct bubbling of gas into the solution or vigorous gas flow at the surface is avoided because of the potential for protein denaturation, which can cause a drift in the optical signal.) The reverse reaction can be carried out on the same sample by switching gas flow back to pure N_2 . Depending on the flow rate, temperature, solution conditions, hemoglobin sample, and hemoglobin concentration, a complete oxygenation reaction with this system requires ~ 20 -30 minutes, and deoxygenation, ~ 40 -60 minutes.

ANALYTICAL PROCEDURES

The spectral data are combined in a single absorbance matrix (A) with a row for each wavelength and a column for each pO_2 . The matrix is reduced to a range from 480-650 nm at 1-nm intervals for a total of 171 wavelengths, or rows (m). The final size of A depends on the number of pO_2 readings, or columns (n), (typically 200-400) to give matrix $A = m \times n$. Two procedures are used for analysis of the A matrix: multicomponent analysis and SVD.

Multicomponent Analysis

Multicomponent analysis determines the composition of a mixture of components when the spectrum of each of the pure parent species is known. The general procedure involves first taking a spectrum of each of the parent species. Second, the spectrum of the mixture is taken. In our case, multiple spectra are taken during the course of a single experiment (*i.e.*, the number of spectra for multicomponent analysis in each experiment is equal to n). Third, a least-squared linear curve-fitting procedure is used to minimize the norm (sum of squares) of the residuals and to obtain the best fit combination of spectra that comprise the mixture. The procedure uses the Moore-Penrose pseudoinverse of a table of the parent spectra (M), where each spectrum is in a separate column. The inversion returns a $p \times m$ matrix (C), where p is the number of parent species. Only C and the experimental spectra (A) are needed for the curve fitting. The procedure is as follows:

- Compute $C = (M^T M)^{-1} M^T$, the Moore-Penrose pseudoinverse of M .

- Compute $P = CA$, where a column of P contains the amounts of the various parent compounds at the corresponding pO_2 . These are normalized to compute percentages.

Parent spectra have been obtained on the rapid-scanning spectrophotometer for oxyhemoglobin (oxyHb), deoxyhemoglobin (deoxyHb), and methemoglobin (metHb). Using these parent spectra to create M , multicomponent analysis is performed on each spectrum (*i.e.*, each column) in A to obtain an estimate of the percentages of oxyHb, deoxyHb, and metHb in each spectrum. Fractional saturation (Y) is calculated from this analysis as,

$$Y = \%oxyHb / (\%oxyHb + \%deoxyHb) \quad (2)$$

in which the percent contribution of metHb is excluded. The change in percent metHb at each step is used to evaluate the rate of change of metHb formation ($\Delta metHb/\Delta t$) as a function of Y . It should be emphasized that these evaluations are only estimates, because to be accurate, the multicomponent analysis procedure must include a parent spectrum for every optical species in the mixed spectrum. To determine the number of optical species in matrix A , SVD is employed.

SVD and Matrix Least Squares

The purpose of this section is to describe two closely related computer-based techniques that place stringent demands on the quality of spectrophotometric data. These techniques are sensitive enough to pick up signals below the noise level of a single spectrum. The trouble is that lamps, gratings, and/or drive chains, as well as experimental designs, can deliver their own signals, which can confound the process one is trying to measure. For example, in the next section, we describe spurious signals that can arise simply because one is doing kinetics (or

"pseudoequilibrium" reactions) instead of step-wise equilibrium, and in the final section, we describe an artifactual spectral component that contributes <0.05% of the total signal.

Let us keep to the context of the oxygenation of hemoglobin as measured by spectrophotometers, although these techniques apply to all manner of spectra and processes.^{29,30} The data consist of a spectrum (from 480 to 650 nm in 1-nm steps to give 171 points in all) collected at each value of pO_2 . As an example, if $\log_{10}(pO_2)$ ranges from -1 to 2 in steps of 0.015, which is 0.1 to 100 mm Hg in increasing steps, 201 complete spectra will be recorded in all. The data are stored in matrix A with 171 rows and 201 columns. Each column of A is a spectrum of hemoglobin at a fixed pO_2 , and each row of A is a hemoglobin oxygenation curve at a fixed wavelength.

The first question is: How many independent spectra and oxygen processes are we looking at? With no notion of chemical mechanism, we can obtain a minimum number of independent spectra necessary to explain all the data. That is, we can find the least number of spectra needed to combine in various ratios to obtain an adequate representation of all the observed spectra. This same number serves as a minimum number of oxygenation processes to explain all the observed titration curves (rows of A). This number is called the rank of A , and there are many ways to estimate it. We chose a standard matrix operation called SVD, because the output from SVD will serve us in other ways. SVD decomposes the matrix A into three factors,

$$A = USV^T, \quad (3)$$

such that

$$U^T U = V^T V = I, \quad (4)$$

and S is diagonal, $s_{1,1} \geq s_{2,2} \geq s_{3,3} \dots$. In our case, the sizes of the factors are

U and S: 171 x 171, V: 201 x 171.

The numbers on the main diagonal of S, sorted in descending order, are the singular values of A. The relations in Eq. (3) enable us to think of A as a sum of a few special components,

$$A = (\text{U column 1})s_{1,1}(\text{V column 1})^T + (\text{U column 2})s_{2,2}(\text{V column 2})^T + \dots \quad (5)$$

The first term of Eq. (5), i.e., $(\text{U column 1})s_{1,1}(\text{V column 1})^T$, is a rank one matrix, the same size as A. But being rank one, it contains only one "spectrum" (U column 1) in its columns, varying only in scale. Likewise, it contains only one "titration curve" (V column 1) in its rows, again varying only in scale. Furthermore, this rank one matrix, of all possible rank one matrices, is the best fit to A in the least-squares sense, and the magnitude of $s_{1,1}$ tells how much of A is explained by this optimal rank one term. Similar descriptions hold for the subsequent rank one terms in Eq. (5), each of which is a best rank one fit to A minus the previous terms. When $s_{i,i}$ is small enough to be regarded as noise, and when (U column i) and (V column i) fail to show anything that looks like signal, we can discard those parts of U, S, and V and keep only the minimal, "noiseless" representation approximating the signal in A. It is this minimal representation property that makes SVD an appealing tool for analyzing complex mixtures. The advantages of this representation are explained in Shrager.³⁰

(At this point, you may want to consult a linear algebra text about matrix multiplication, transpose, diagonal, identity, inverse, and the Frobenius norm, which we will refer to as norm.) The norm of S is the same as the norm of A. You can estimate the rank of A by plotting $\log_{10}(s_{i,i})$ versus i , most of which will be a smooth curve, almost a straight line for small i , except for the first few values. These will stand out above the others as signal stands out above noise, and the number of these standouts will estimate the rank. Sometimes, it is difficult to decide

where the standouts end, which is appropriate. The difficulty provides a sense of doubt about concepts such as rank. One should not put too much confidence in computations that produce integer answers (decisions, if you will) from data with a continuous range of possible values. Alternate and possibly conflicting ways of estimating rank are provided in previous publications.^{29,30} Rank becomes a working hypothesis, not a "hard" number.

Having chosen a rank r , we can now express our goal in matrix terms. We wish to decompose the matrix A into two factors,

$$A = DF^T \quad (6)$$

where D is a $171 \times r$ matrix, its r columns containing the spectra that are changing. The columns of D are plotted *versus* wavelength. F is a $201 \times r$ matrix of appearance-disappearance curves for the spectra in D . The columns of F are plotted *versus* $\log_{10}(pO_2)$.

Just as you must know two of the three numbers when solving the scalar equation $ab = c$, likewise, you must know two of the three matrices when solving $A = DF^T$. By using computer modeling in conjunction with least squares, one can often obtain a good estimate of F (an example of how F is chosen is given below) and then compute D by the formula $D = A(F^{T+})$, where (F^{T+}) is the Moore-Penrose pseudoinverse of (F^T) .³¹ This process is called matrix least squares, and programs for carrying it out directly, without going through the intermediate SVD steps described below, are described in Frans and Harris.³² The relation between $A = DF^T$ (the matrix least-squares decomposition) and $A = USV^T$ (the SVD) is given by,

$$V^T = H F^T \quad (7)$$

and

$$D = USH \quad (8)$$

where H is found by making successive guesses at the Adair parameters that determine F , generating F , then applying matrix least squares,

$$H = V^T(F^{TT}) \quad (9)$$

The solution parameters are those that minimize the norm of $S(V^T - HF^T)$.

This SVD-based procedure is proven in Shrager³⁰ to give exactly the same result as direct matrix least squares. So what are the reasons for using SVD? One reason is that the full U , S , and V matrices are in fact never used, because statistically indistinguishable results can be obtained by using only the first r columns of U and V , and the first r rows and columns of S . Thus, in terms of computing effort, $V^T = HF^T$ is a much smaller problem than $A = DF^T$. But equally important, SVD offers assistance in choosing a feasible model. Trying to derive a model by looking at the rows of A is often difficult, because the rows of A tend to look alike in a restricted wavelength region, and because small but independent trends tend to be swamped by larger trends and even by noise in any single row of A . But SVD has two advantageous properties. First, SVD collects almost all the signal in all the rows of A into the fewest possible columns of V (e.g., in our experiments, we rarely have to look past the fifth column in V for signal). Second, SVD tends to produce columns of V of contrasting shape, so that if a small but significant trend does not show up well in one column of V , it shows up well in another. These contrasting shapes also convey information about mechanism. If there are only two spectra in the data (e.g., deoxyHb and oxyHb with no distinction between T and R states), then the apparent rank of A will be $r = 2$, and only the first two columns of V will have significant signal. Furthermore, both columns will follow the Adair trend, a single sigmoid, with contrast only in the base level and scale of the curves. (F in this case consists of two Adair curves: 0 to 1 and

1 to 0.) But if, say, there are four distinguishable species: deoxy T, deoxy R, oxy T, and oxy R, then four columns of V will contain signal, and their number of up-and-down trends *versus* pO_2 will absolutely preclude a simple deoxy-to-oxy mechanism.

So now the question is: for a four-species model, what can we use in place of the Adair curves in F? The Adair curves were in F because the 0-to-1 curve described the appearance of oxyHb, and the 1-to-0 curve described the disappearance of deoxyHb. Now we must describe the appearance and disappearance of four species (*i.e.*, species = type of site: unbound T or R, or bound T or R) by postulating models and testing them. For a simple example, assume that all hemoglobin tetramers are in the T state for zero sites or any one site bound to oxygen and in the R state for any two, three, or four sites bound, with no distinction between the α and β sites. By the laws of mass action, the populations of the four species (sites) are:

$$\text{Let } x = pO_2,$$

$$D = 1 + a_1x + a_2x^2 + a_3x^3 + a_4x^4,$$

$$y_i = \text{concentration of Hb}(O_2)_i, \text{ (i.e.,}$$

$$y_0 = 1/D, \text{ and}$$

$$y_i = a_ix^i/D, i = 1:4). \text{ Then the desired populations are:}$$

$$\text{deoxy T} = y_0 + 0.75y_1$$

$$\text{oxy T} = 0.25y_1$$

$$\text{deoxy R} = 0.5y_2 + 0.25y_3$$

$$\text{oxy R} = 0.5y_2 + 0.75y_3 + y_4.$$

So, as expected, the oxygenation model will start at $x = 0$ with all deoxy T, finish at high x with almost all oxy R, with oxy T and deoxy R as rising and falling intermediates. These are the four

columns of F , the shapes of which are governed by the a 's, which are adjusted by a curve-fitting program to minimize the norm of $A - DF^T$ (in full matrix least squares) or $S(V^T - HF^T)$ (in the SVD-based procedure). The choice of model depends on the combination of intermediates in the two conformational states and can be tested by allowing for the best fit to the data.

The differences between T and R spectra are subtle at best. Only a sensitive procedure can hope to detect them. And since we are using least squares rather than partial least squares, our model must include any phenomenon that our procedure can detect, not only T to R transitions, but also metHb formation and dimerization, unless these effects can be stabilized. (With some reformulation of the problem, SVD can ignore unchanging background.) But to return to the original point, if our instruments (*e.g.*, spectrophotometers and electrodes), our data scrubbing (*e.g.*, digital filters), or our experimental designs (*e.g.*, kinetics with slow spectrophotometric scans) introduce subtle signals of their own, analysis becomes more difficult.

Kinetics and the spectrophotometer: a study in artifact

The purpose of this section is to provide some corrections for errors induced by slow kinetics (*i.e.*, "pseudoequilibrium") rather than step-wise equilibrium. Time must be recorded along with pO_2 , absorbance, and even wavelength in some cases. Spectra take time to gather. When the wavelength range is scanned, absorbance at each wavelength is measured at a different time. When several such spectra are averaged, the distribution of sample times is unique for each wavelength. To specify this distribution, some notation is in order:

n = number of scans combined to produce a single spectrum.

Wavelength:

w = wavelength in nm.

w_{\min} = minimum wavelength (start of a forward scan).

w_{\max} = maximum wavelength (start of a backward scan).

w_c = central $w = (w_{\min} + w_{\max})/2$.

Time:

t = time in some standard unit.

t_i = time to scan from w_{\min} to w_{\max} , forward or backward.

t_d = dead time between successive scans.

t_c = central t , midway between the start of scan 1 and the end of scan n , including dead times. For all computations below, $t_c = 0$ should be used to improve the condition of the matrices involved.

c_i = central time of the i^{th} scan relative to t_c .

$f(w)$ = time of sample of w relative to w_c in a forward scan.

$b(w)$ = time of sample of w relative to w_c in a backward scan.

$t_i(w)$ = time of sample of w in the i^{th} scan relative to t_c .

Absorbance:

a = absorbance in optical density.

$a(w, t_i(w))$ = observed a from the i^{th} scan at w (and $t_i(w)$).

$a(w, t_c)$ = estimated a at w and t_c , (i.e., a deduced simultaneous spectrum at t_c , corrected for time dependence).

$a'(w, t_c)$ = the first time derivative, $da(w, t_c)/dt$.

$a''(w, t_c)$ = the second time derivative, $d^2a(w, t_c)/dt^2$.

Our focus in this context is $a(w, t_c)$, but what we obtain from the scanning procedure is a series of spectra,

$$a(w, t_i(w)) = a(w, t_c) + a'(w, t_c)t_i(w) + 1/2a''(w, t_c)t_i^2(w) \quad (10)$$

which, even when averaged, do not produce the desired spectrum. Equation (10) is a three-term Taylor series expansion of $a(w, t_c)$ with respect to time. (If the scan is so slow that three terms are not enough, chances are that the wrong experiment is being performed.) Using formula (10) as a model, time effects can be corrected for by fitting the curve $a(w, t_i(w))$ versus $t_i(w)$ to a parabola at each fixed w . One needs at least three scans to do this because there are three parameters, but 10 scans or more are preferred to reduce noise. To do any of this, the functions $t_i(w)$ must be known. The linear model of $t_i(w)$ is offered here as simple to apply, but a more realistic model is to be preferred:

$$t_i(w) = t_c + c_i + f(w), \text{ where}$$

$$c_i = [i - (n+1)/2](t_s + t_d), \text{ and} \quad (11)$$

$$f(w) = t_i(w) - c_i = (t_s/2)(w - w_c)/(w_{max} - w_c).$$

As suggested above, $t_c = 0$ should be the convention in Eqs. (11). From Eqs. (11), for any wavelength, all the times at which $a(w, t)$ was sampled can be generated. Fitting a parabola versus t to a parabola and picking off $a(w, t_c)$ is then standard procedure. Also, when all scans are forward, the $t_i(w)$ are spaced equally, and the spacing $t_s + t_d$ is the same for all w , although the time displacement from t_c is not. Still, the common spacing allows for considerable economy of calculation, because only one matrix need be inverted instead of one for each w , i.e.,

$$G = \left\{ \begin{bmatrix} 1 & 1 & \dots & 1 \\ t_1(w) & t_2(w) & \dots & t_n(w) \\ t_1^2(w) & t_2^2(w) & \dots & t_n^2(w) \end{bmatrix}' \right\}^* \quad (12)$$

For each w ,

$$h = G[a(w, t_1(w)) \ a(w, t_2(w)) \ \dots \ a(w, t_n(w))]', \text{ and}$$

$$a(w, t_c) = h_1 - h_2 f(w) + h_3 f^2(w).$$

In matrix (12), the $*$ symbol once again stands for the Moore-Penrose pseudoinverse, this time of an $n \times 3$ matrix. G itself will be a $3 \times n$ matrix.

Some spectrophotometers allow both forward and backward scans. We will assume that the timing of a backward scan is symmetric to the timing of a forward scan [i.e., $b(w) = -f(w)$]. If the forward-backward feature is used, successive scans should alternate in direction, and the number of scans should be even to cancel out the effects of odd terms in the Taylor series in formula (10). When this is done, the central time, t_c , is also the midrange time $[t_1(w) + t_n(w)]/2$ for every w , but the spacings of $t_i(w)$ are different for every w . In particular, for w linear in t within each scan, we have:

$$t_i(w) = t_c + c_i + f(w) \text{ for odd } i, \text{ and}$$

$$t_i(w) = t_c + c_i - f(w) \text{ for even } i, \text{ where} \quad (13)$$

$$t_c, c_i, \text{ and } f(w) \text{ are as defined in (11).}$$

This staggered spacing of $t_i(w)$ requires a different matrix-inverse for every w , but because of symmetric properties, rows two and three of G become superfluous. The procedure for interpolating $a(w, t_c)$, including computing G , is repeated for every w :

$$G = \left\{ \begin{bmatrix} 1 & 1 & \dots & 1 \\ t_1^2(w) & t_2^2(w) & \dots & t_n^2(w) \end{bmatrix} \right\} \quad (14)$$

$$H = [a(w, t_1(w)) \quad a(w, t_2(w)) \quad \dots \quad a(w, t_n(w))]'$$

$$a(w, t_c) = [G \text{ row } 1] H$$

Of course, the collection of [G row 1]'s for all w will be constant for any sampling pattern, not only for all t in the current experiment, but also for other similar experiments. So rather than recompute G every time it is needed, one may choose to store all the [G row 1]'s in a file, and retrieve them, or compute them for the first t_c , and keep them in memory for subsequent t_c . The choice will depend on n , the number of w , and the memory capacity and speed of the computer.

When several "instantaneous" scans (e.g., from a photodiode array) are being combined to produce the spectrum at t , formulas (13,14) can still be used, with the following simplification: $f(w) = 0$, and consequently, the same [G row 1] holds for all w .

When several scans are combined to produce a single spectrum, one may assume that errors due to the length of a single absorbance measurement are negligible compared with the discrepancies between scans. But when all measurements are taken at once, as in a photodiode array, one may decide on a single long scan to reduce noise, rather than combine several short scans. The errors now take on a new disguise: an integral. Taking t_c to be zero, a scan runs from $-t_s/2$ to $t_s/2$, common to all w . The result is an average value over that interval, namely,

$$\bar{a}(w, 0) = 1/t_s \int_{-t_s/2}^{t_s/2} [a(w, 0) + a'(w, 0) t_s + 1/2 a''(w, 0) t_s^2] dt \quad (15)$$

again limiting the Taylor expansion in the integrand to three terms. From Eq. (15), we can deduce the following correction:

$$a(w, t_c) = \bar{a}(w, t_c) - 1/24 a''(w, t_c) t_c^2 \quad (16)$$

Unlike the multiple-scan situation, where several samples are available for least-squares approximation of $a(w, t)$, in Eq. (16) there is no local information except $\bar{a}(w, t_c)$. This single datum cannot be used to correct itself. A less local approach must be used to approximate a'' for the correction in Eq. (16). One method is to fit a local parabola through $\bar{a}(w, t_c)$ and its neighbors in time, and use that second derivative as a'' . Another method is to use a global model (e.g., the Adair curve) for all t_c , and use the second derivative of that model fitted to data at each wavelength.

Do we accomplish anything by these corrections? Remember, the corrections are being made because the data will be subjected to highly sensitive analysis methods. If, for example, the SVD analysis reveals unexplained components in the raw data $\bar{a}(w, t_c)$, and if these components disappear when the data are corrected, one can be fairly certain that they are artifacts of time dependence.

In our case, the need for a derivative correction was eliminated by doing alternate forward and backward scans. By numerically approximating second derivatives, it was determined that the corrections would be well below any effect we could measure, including noise, and so the correction procedure was not used in the experiments that we will now describe.

AN EXAMPLE OF THE EXPERIMENT

A representation of an experimental matrix A is shown in Fig. 2. In this experiment, human deoxyhemoglobin in 50 mM bis-Tris, 0.1 M Cl^- , at pH 7.4 was oxygenated at 25°C. Matrix A was evaluated by SVD to determine the rank, r , of the matrix and to construct the

matrices U , S , and V , where the columns in U are linear combinations of the independent spectra of each component in A , the columns of V are linear combinations of the transitions of each component in A , and S is used to evaluate r , or the number of components necessary to generate A . For ideal data (i.e., the absence of noise), r is given by the number of nonzero diagonal elements in S . For real data, all the diagonal elements of S are positive, but the values that are derived from noise are small. The chemical transitions that are resolved by SVD are above the noise level. For columns i where $i > r$, U column i and V column i contribute a negligible amount to the signal in A .

Analysis of the rank of A is shown in Fig. 3. In this experiment, a maximum of five spectral components are attributed to A , and the first five columns of matrices U and V from this example are represented in Figs. 4(A-E). The increasing contribution of noise is evident as we move from the lower to higher numbered columns in U and V . As shown by the singular values in Fig. 3, the first two components comprise the large majority of the signal. Inspection of U columns 1 and 2 shows that the first component reflects primarily the linear average of the deoxyHb and oxyHb spectra in the matrix, and the second component reflects primarily the oxyHb-deoxyHb difference spectrum. The transitions of both of the major components, as shown in V columns 1 and 2, are sigmoid curves and reflect the oxygen binding equilibrium. The other three components have much smaller contributions to the overall transition, and as expressed by the ratio of their singular value to the sum of the first and second component singular values, the fractions of the signal contributed by the third, fourth and fifth components are ~0.084%, ~0.040% and ~0.032%, respectively.

A first approximation of the identity of the third component, if we assume that some of the heme-iron atoms oxidized during the experiment, is made by multicomponent analysis of matrix **A** based on three species, deoxyHb, oxyHb, and metHb. This analysis is only a first-order approximation because its accuracy depends on the completeness of matrix **M**, containing a parent spectrum for every species in the experimental data, but by SVD, the rank of **A** is probably greater than three. Even so, the minor two components are near the level of random noise and comprise a total of less than one part in 1000 of the entire spectral information in **A**. In this case, multicomponent analysis provides a reasonable evaluation of the percentage of deoxyHb, oxyHb, and, to a lesser extent, metHb in each spectrum of **A**. Fractional saturation, **Y**, is calculated from Eq. (2), and the rate of change of metHb ($\Delta\text{metHb}/\Delta t$) can be examined according to this analysis in relation to **Y** (Fig. 5). It can be seen that the position of the $\Delta\text{metHb}/\Delta t$ maximum is similar to that in the transition of **V** column 3.

The fourth SVD component shows a transition having some $p\text{O}_2$ -correlation resolved just above random noise. It is difficult to interpret this signal, however, because it is so small. For the type of experiment described here, instrument noise must be decreased or the signal must be enhanced before matrix least-squares analysis can be used to model this transition successfully.

The fifth SVD component is wholly or partially an instrumental artifact that has primarily random correlation with $p\text{O}_2$. The signal is revealed as a derivative of the parent spectra that arises due to slight fluctuations in wavelength position from scan to scan. The error is too small to be seen visually, but because it results from a non-random signal, it is resolved by SVD.

Wavelength-position error can be detected by repeated scanning of a static sample having a sharp peak, such as oxyhemoglobin, carbonmonoxyhemoglobin, or reduced cytochrome c. For

the highest reproducibility of repeated scans, the sample should be scanned as fast as possible to avoid problems of protein deterioration or changes in ligand or oxidative state. Theoretically, in the absence of horizontal wavelength "jitter", SVD analysis of repeated scans of a static sample will produce a single component above the random noise of the system. Alternatively, a second SVD component in this analysis will provide the contribution of the error as $s_{2,2}$ and the derivative spectrum as U column 2.

The primary obstacle in the modeling effort now is in the derivation of an appropriate model for the transition to methemoglobin. Multicomponent analysis gives us an approximation of methemoglobin formation in relation to hemoglobin saturation (*i.e.*, see Fig. 5), but it does not reveal the mechanism of oxidation in the tetramer, which may occur at any one of four binding sites, to any partially liganded species, and, perhaps, preferentially at one type of subunit. The reaction becomes notably more complex with these considerations, and modeling it is nontrivial. Information about the process of hemoglobin oxidation is required for a realistic model. As a first step, valency hybrids can be used to evaluate the effects of oxidation on the equilibrium curve.³³

The hemoglobin conformational transition, which can be resolved as a singular spectral component if the signal measurement is sensitive and accurate enough, is another area under study. Strong allosteric effectors, such as inositol hexaphosphate²⁸ and bezafibrate, are being used to test this by possibly enhancing the signal. Alternatively, since the extinction coefficient for the quaternary change is much higher in the Soret region,¹⁵ there is a better probability of detecting this signal between 410 and 450 nm by using a lower heme concentration in our

reaction cell or by using the shorter path length of the thin-layer apparatus in a rapid-scanning spectrophotometric system.²⁵

In the future, mathematical models will include calculations of tetramer dissociation and, perhaps, subunit differences in ligand binding. As instruments and theory improve, the critical components of the reaction will be resolved better, and once limiting assumptions are no longer required for experimental analyses, the evaluation of hemoglobin-oxygen equilibrium binding will become a simpler and more reliable process.

Authors' note:

The opinions or assertions contained herein are the private views of the authors and are not to be construed as official or as reflecting the views of the U.S. Department of the Army or the Department of Defense.

REFERENCES

- ¹ G.S. Adair, *J. Biol. Chem.* 63, 529 (1925).
- ² J. Monod, J. Wyman, and J.P. Changeux, *J. Mol. Biol.* 12, 88 (1965).
- ³ M.F. Perutz, *Nature* 228, 726 (1970).
- ⁴ G.K. Ackers, M.L. Doyle, D. Myers, and M.A. Daugherty, *Science* 255, 54 (1992).
- ⁵ M. Perrella and L. Rossi-Bernardi, *Meth. Enzymol.*, this volume [48].
- ⁶ F.C. Mills, M.L. Johnson, and G.K. Ackers, *Biochemistry* 15, 5350 (1976).
- ⁷ K. Imai, *Meth. Enzymol.* 76, 438 (1981).
- ⁸ J.S. Olson, M.E. Anderson, and Q.H. Gibson, *J. Biol. Chem.* 246, 5919 (1971).
- ⁹ A. Nasuda-Kouyama, H. Tachibana, and A. Wada, *J. Mol. Biol.* 164, 451 (1983).
- ¹⁰ Q.H. Gibson, *Biochem. J.* 71, 293 (1959).
- ¹¹ M. Brunori, E. Antonini, J. Wyman, and S.R. Anderson, *J. Mol. Biol.* 34, 357 (1968).
- ¹² M.L. Adams and T.M. Shuster, *Biochim. Biophys. Res. Comm.* 58, 525 (1974).
- ¹³ C.A. Sawicki and Q.H. Gibson, *J. Biol. Chem.* 251, 1533 (1976).
- ¹⁴ J. Hofrichter, J.H. Sommer, E.R. Henry, and W.A. Eaton, *Proc. Natl. Acad. Sci. U.S.A.* 80, 2235 (1983).
- ¹⁵ A. Bellelli and M. Brunori, *Meth. Enzymol.*, this volume [32].
- ¹⁶ M.L. Johnson, *Meth. Enzymol.*, this volume [54].
- ¹⁷ A. Hayashi, T. Suzuki, and M. Shin, *Biochim. Biophys. Acta* 310, 309 (1973).
- ¹⁸ C.C. Winterbourn, B.M. McGrath, and R.W. Carrell, *Biochem. J.* 155, 493 (1976).
- ¹⁹ K. Imai, *Meth. Enzymol.*, this volume [52].
- ²⁰ F.J.W. Roughton, *Biochem. J.* 29, 2604 (1935).
- ²¹ J. Rifkind and R. Lumry, *Fed. Proc.* 26, 2325 (1967).

- ²² K. Imaizumi, K. Imai, and I. Tyuma, *J. Biochem.* **83**, 1707 (1978).
- ²³ L.J. Parkhurst, T.M. Larsen, and H.-Y. Lee, *Meth. Enzymol.*, this volume [56].
- ²⁴ M.L. Doyle, E. Di Cera, and S.J. Gill, *Biochemistry* **27**, 820 (1988).
- ²⁵ D.W. Ownby and S.J. Gill, *Biophys. Chem.* **37**, 395 (1990).
- ²⁶ T.M. Larsen, T.C. Mueser, and L.J. Parkhurst, *Anal. Biochem.* **197**, 231 (1991).
- ²⁷ R.M. Winslow, A. Murray, and C.C. Gibson, *Meth. Enzymol.*, this volume [50].
- ²⁸ K.D. Vandegriff, Y.C. Le Tellier, J.R. Hess, and R.I. Shrager, *Biophys. J.* **61**, A55 (1992).
- ²⁹ R.I. Shrager and R.W. Hendler, *Anal. Chem.* **54**, 1147 (1982).
- ³⁰ R.I. Shrager, *Chemomet. & Intell. Lab. Sys.* **1**, 59 (1986).
- ³¹ G. Golub and W. Kahan, *SIAM J. Num. Anal. (B)* **2**, 205 (1965).
- ³² S.D. Frans and J.M. Harris, *Anal. Chem.* **56**, 466 (1984).
- ³³ M.C. Marden, J. Kister, and C. Poyart, *Meth. Enzymol.*, this volume [33].

FIGURE LEGENDS

Fig. 1: Schematic diagram of the experimental system for rapid-scanning analysis of hemoglobin-oxygen equilibrium binding. Details are provided in the text.

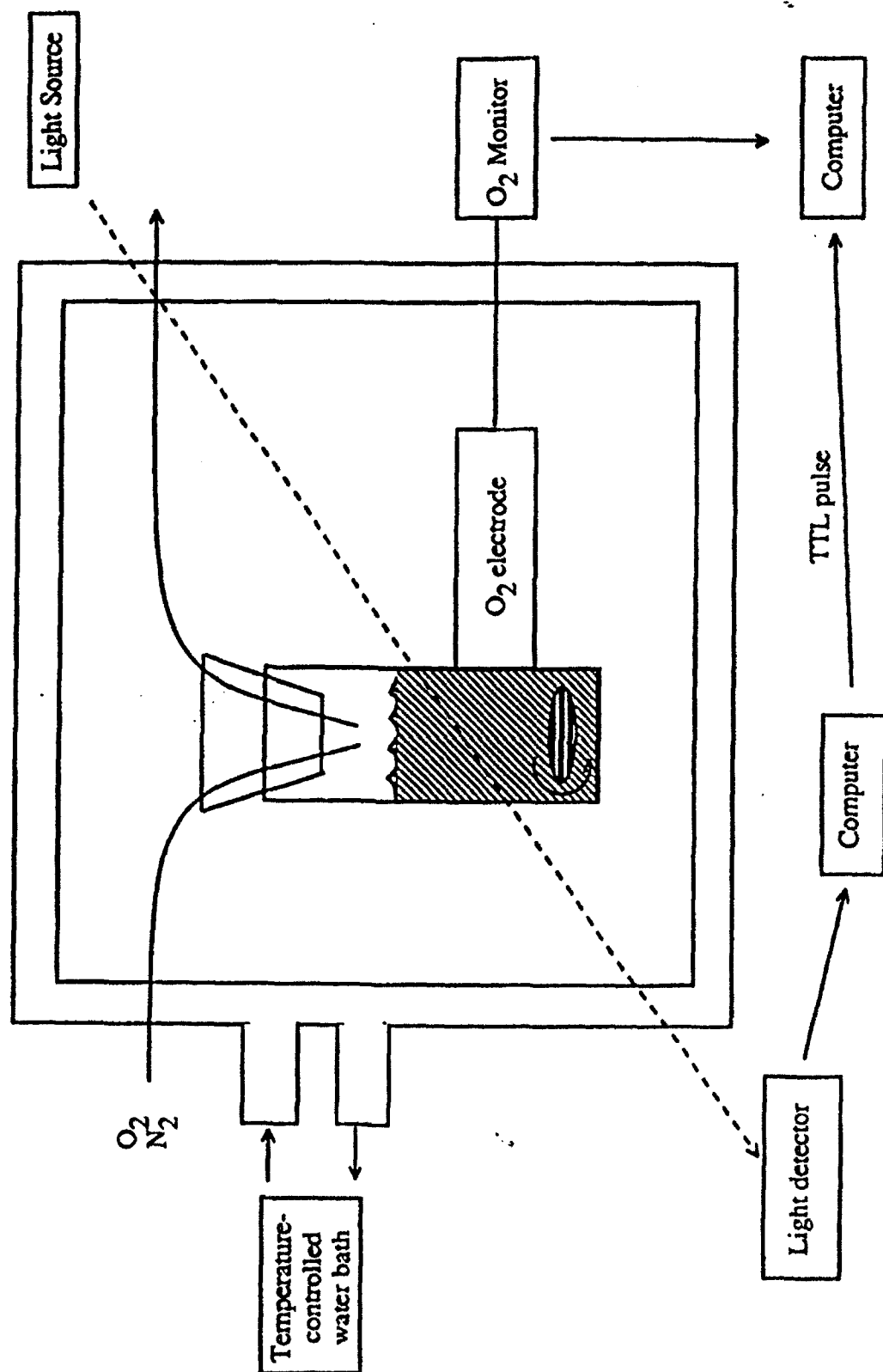
Fig. 2: Matrix A. Wavelength is shown along the x-axis from 480-650 nm. Absorbance units (Au) are given on the y-axis (maximum absorbance ≈ 1 Au), and pO_2 in mm Hg is shown increasing along the z-axis from 0 to ~ 100 mm Hg. For clarity, only every fifth data point is represented along the z-axis.

Fig. 3: Evaluation of the rank of A. Singular values from the diagonal matrix S as determined by SVD of matrix A. Only the first 50 values are represented. The rank of matrix A is estimated as five by identification of five component singular values above the systematic decline in $\log_{10}(s)$.

Fig. 4: The first five columns of matrices U and V by SVD of matrix A. U (top) and V (bottom) columns (A) 1, (B) 2, (C) 3, (D) 4, and (E) 5.

Fig. 5: Oxygen equilibrium curve (o) and rate of change in percentage of metHb ($\Delta\text{metHb}/\Delta t$) (---) from the binding reaction of human hemoglobin. Conditions: 60 μM (in heme) human hemoglobin A_0 in 50 mM bis-Tris, 0.1 M Cl^- , pH 7.4 at 25°C. Symbols give fractional saturation (Y) as a function of pO_2 in mm Hg. The line (---) represents a smoothed, five-fold magnification in amplitude of $\Delta\text{metHb}/\Delta t$ as a function of pO_2 . "Y" was calculated from Eq. (2), using the multicomponent analysis of matrix A from three parent species, oxyHb, deoxyHb, and metHb. ΔMetHb was calculated as the percentage change in metHb from spectrum to spectrum as determined by multicomponent analysis of matrix A.

Fig. 1



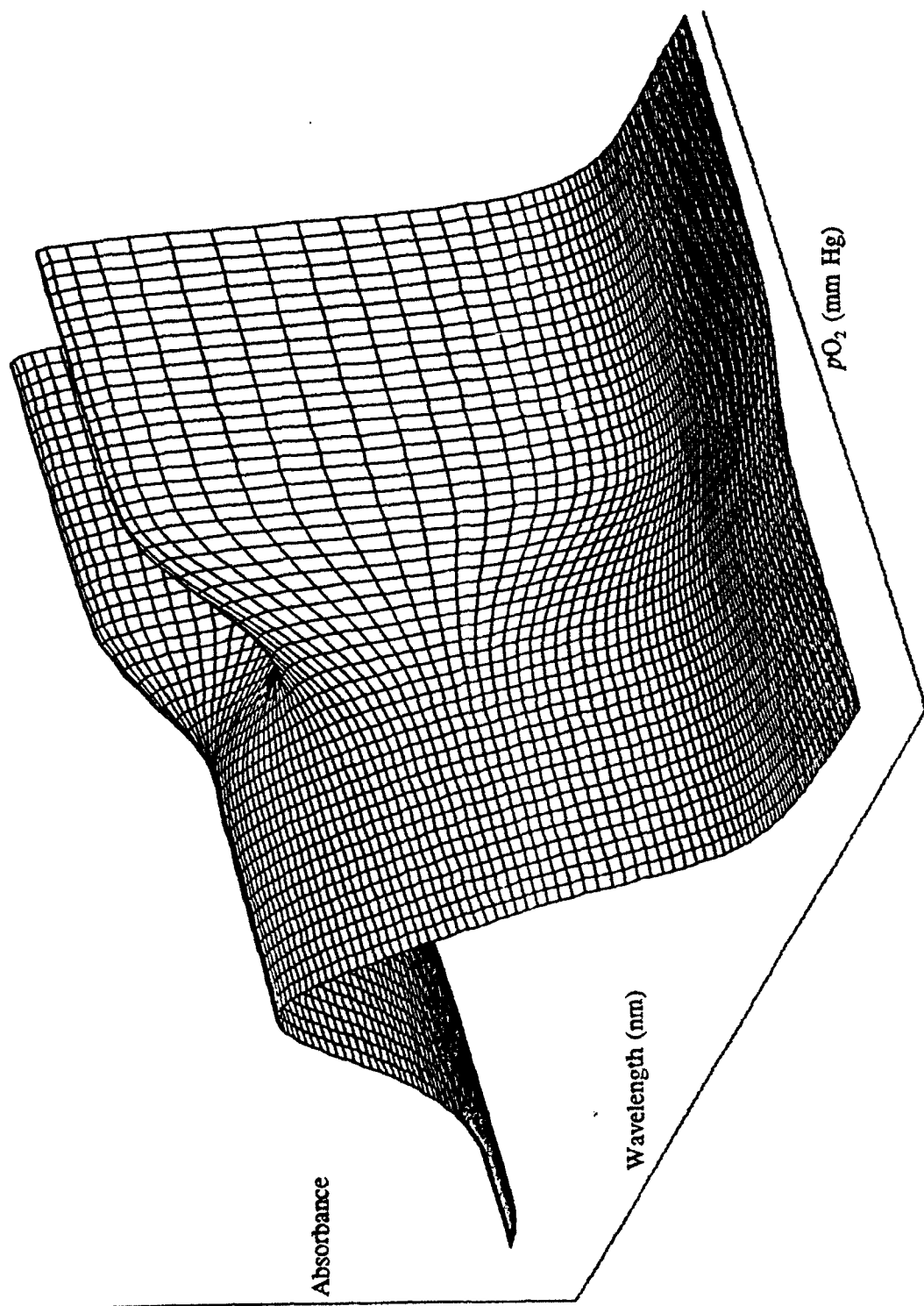
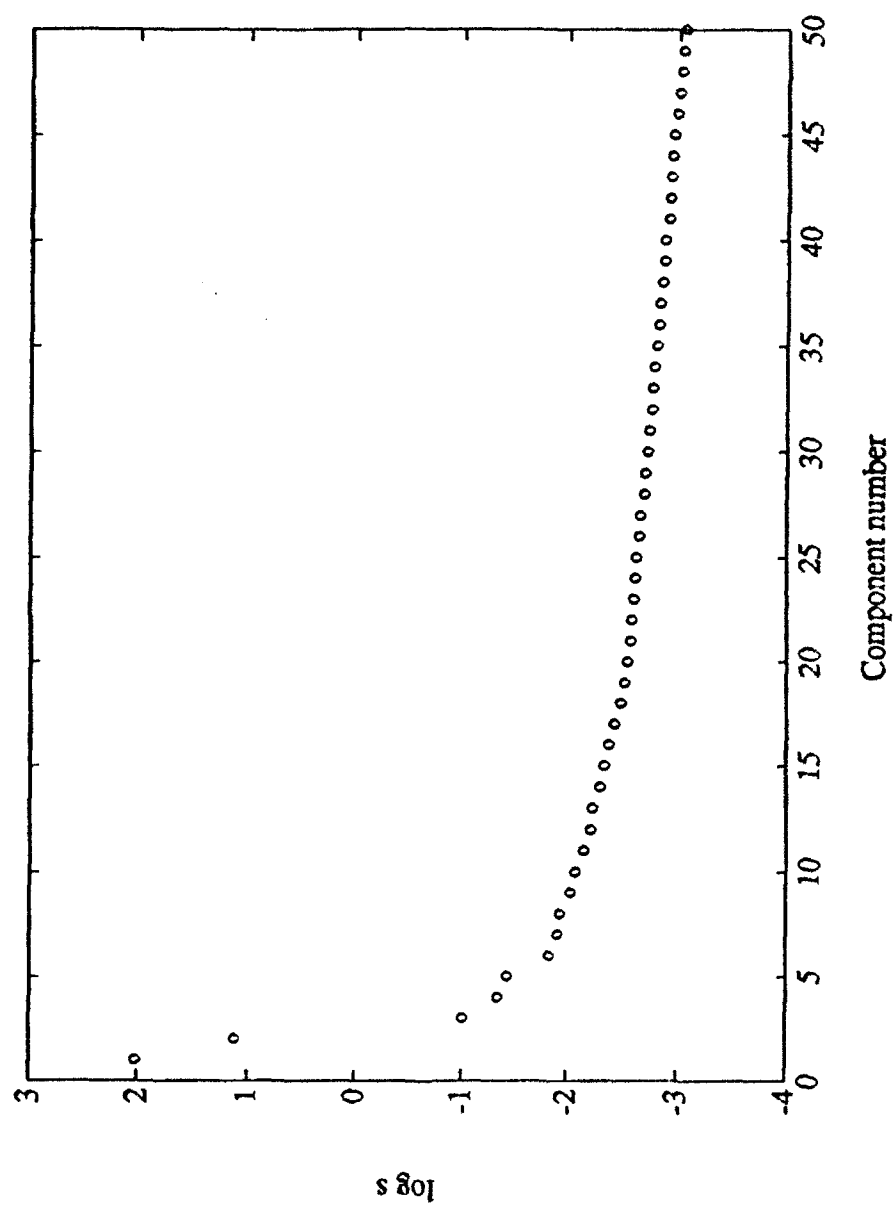
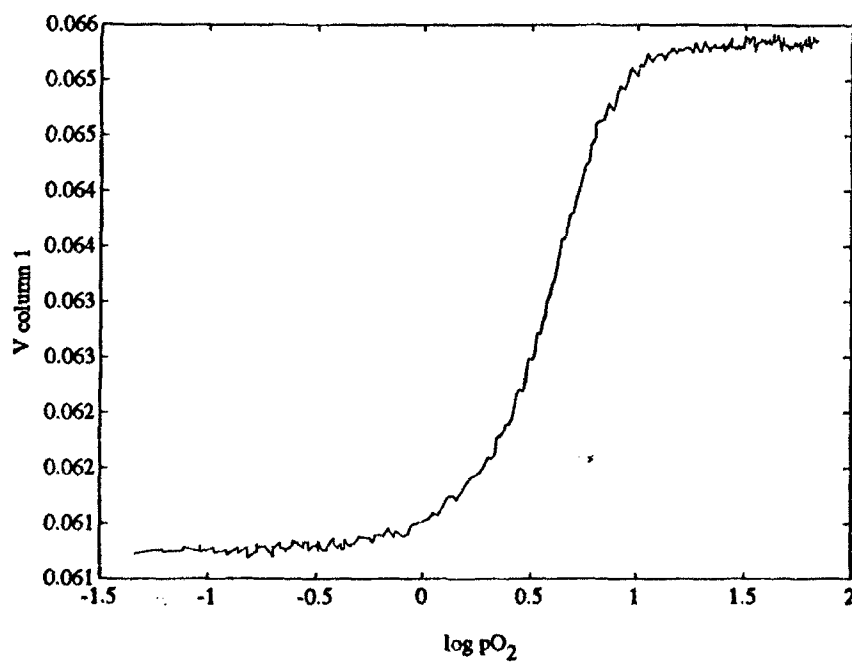
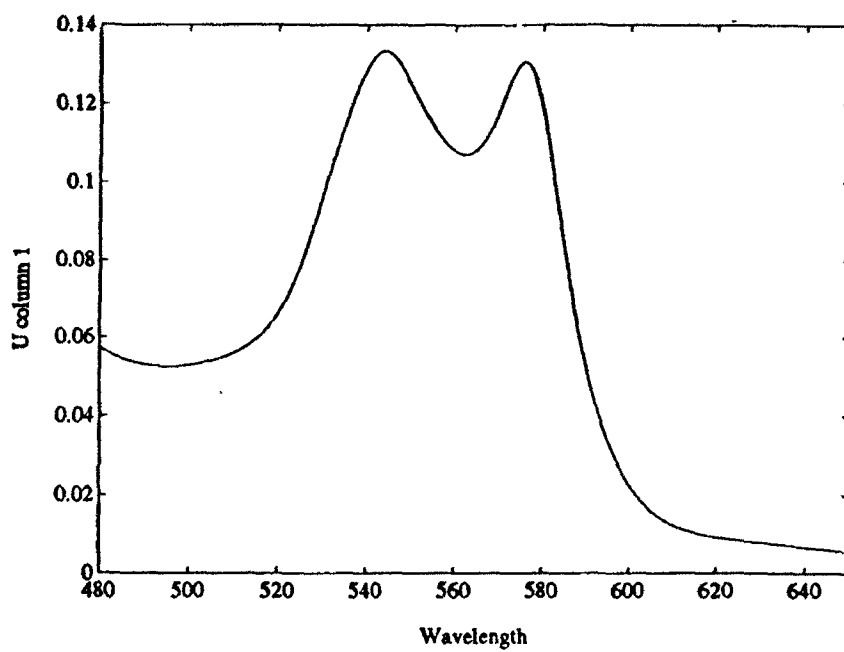
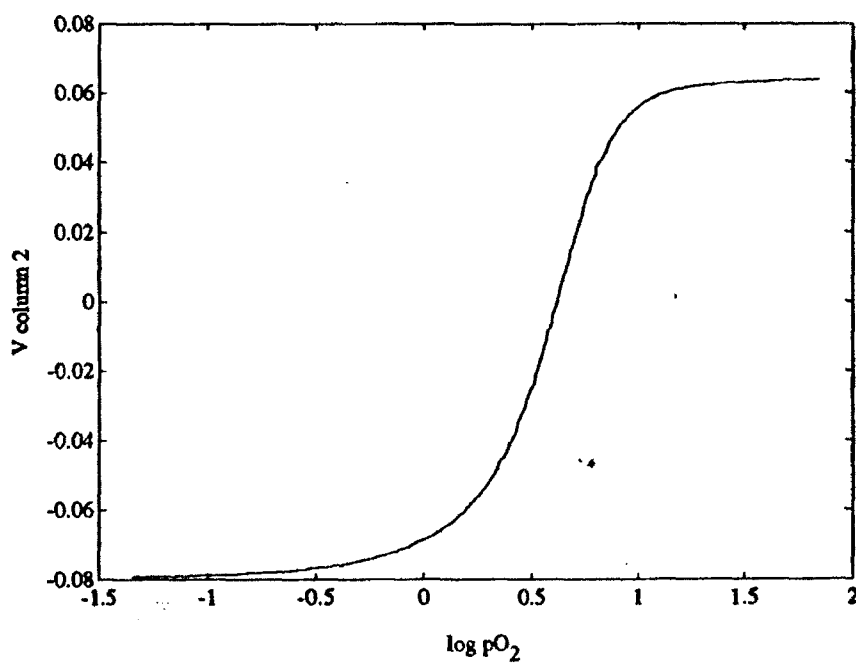
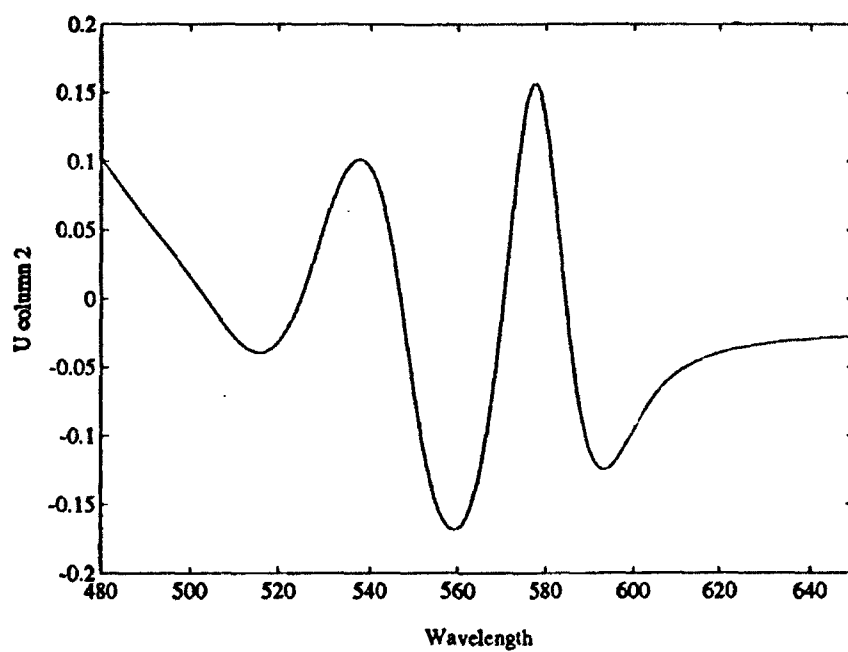
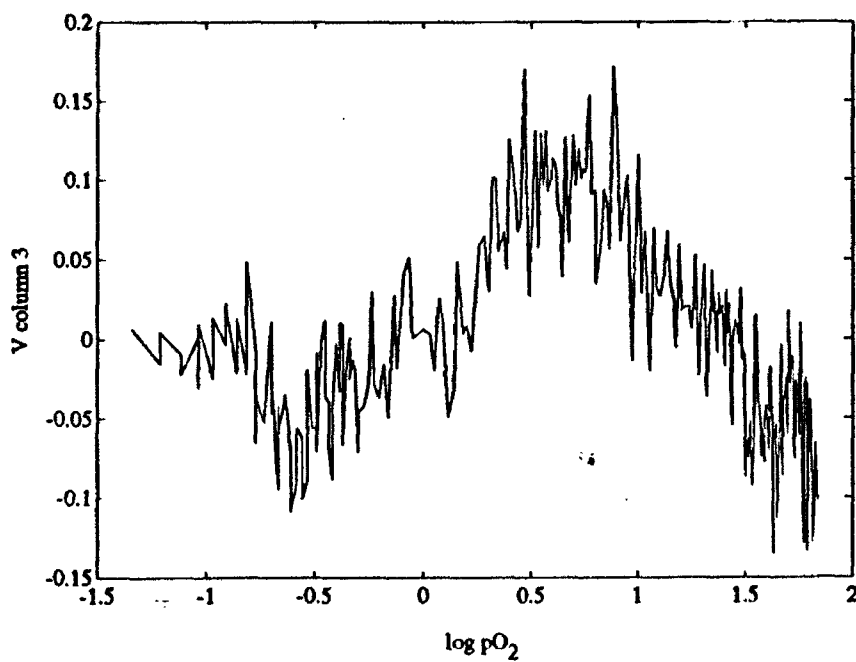
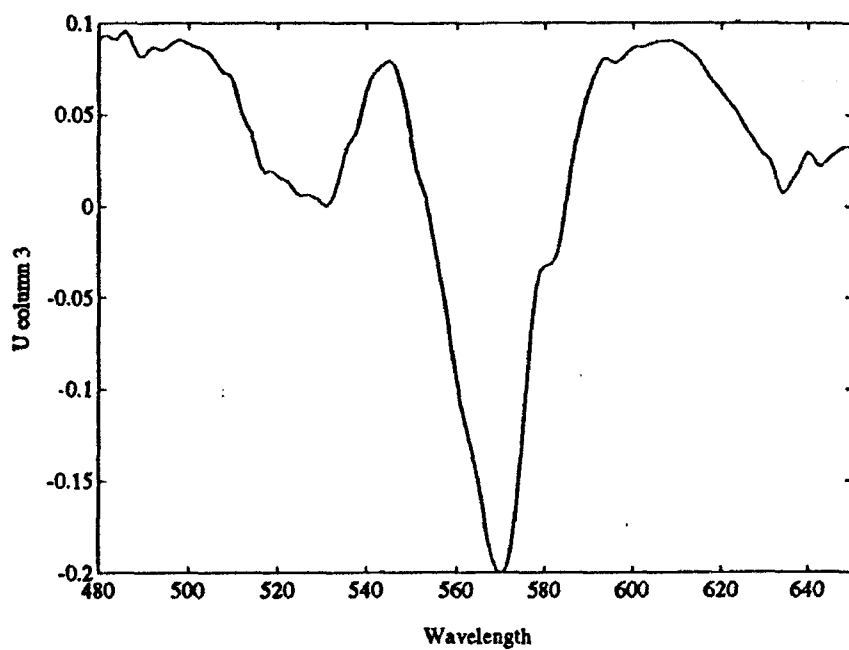


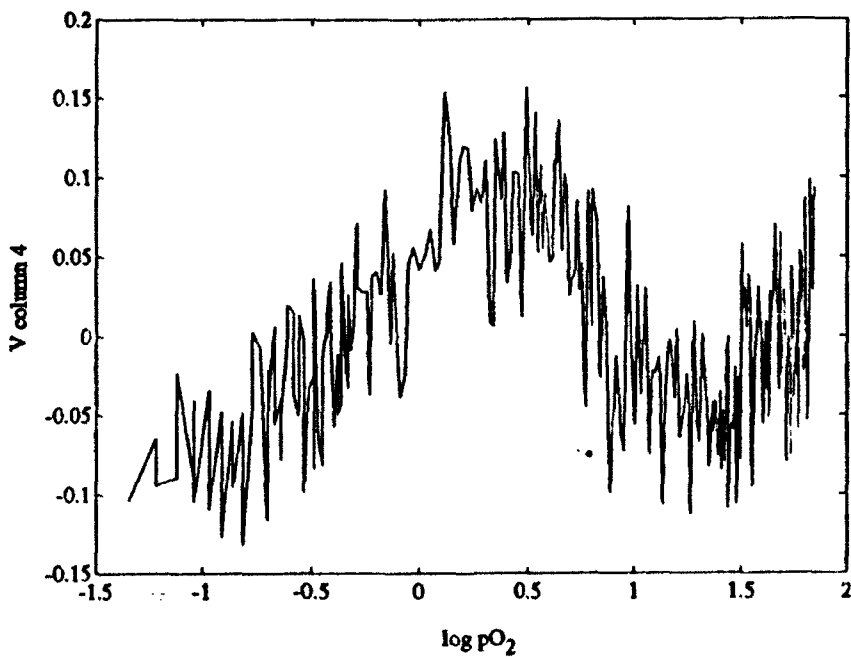
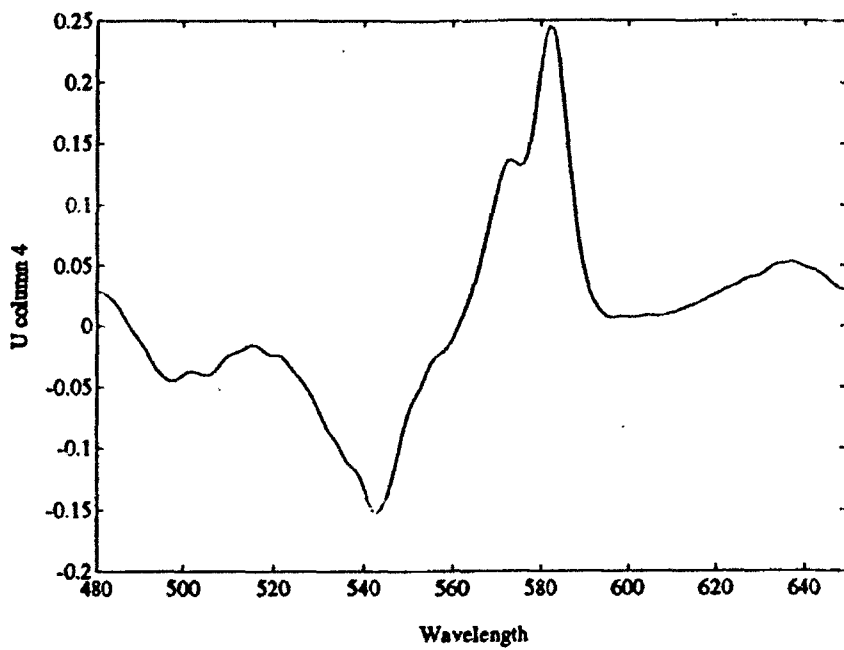
Fig. 3











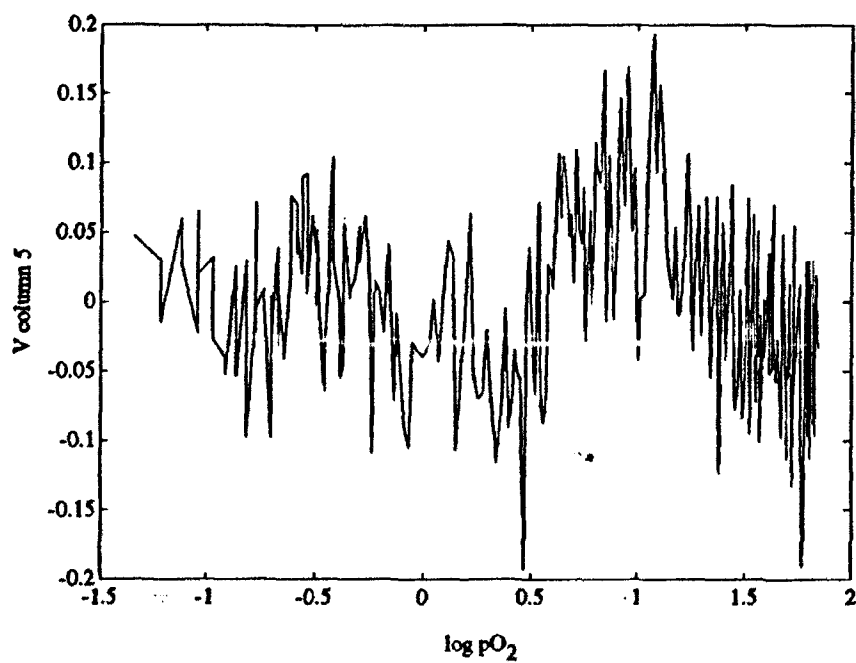
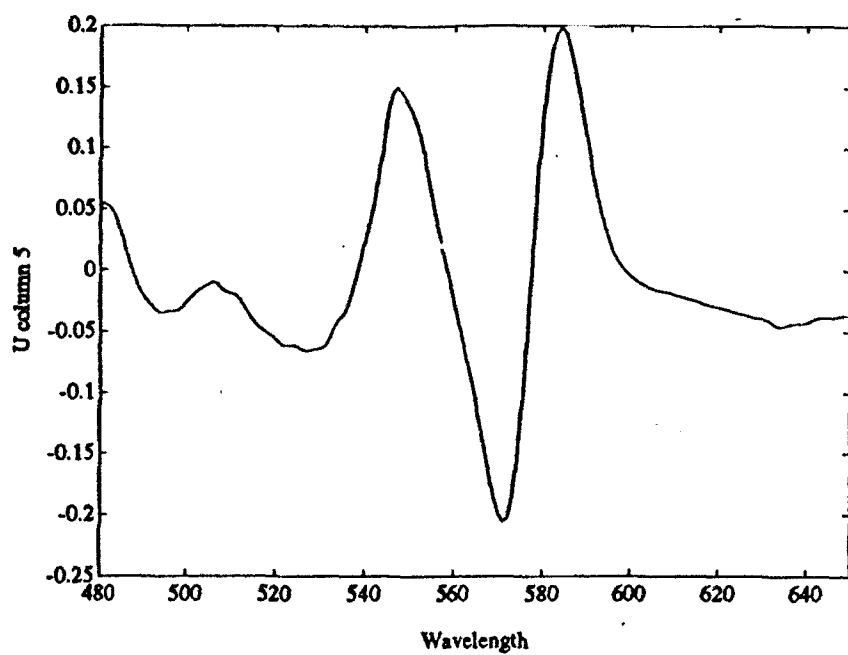


Fig. 5

